Vol.16 No.3, 2014

Original Paper

Multidimensional Matching of Tactile Sensations of Materials and Vibrotactile Spectra

Yoichiro Matsuura, Shogo Okamoto, Hikaru Nagano, and Yoji Yamada*1

Abstract – Specifying the relationship between the sensations perceived by material surfaces and the tactile stimuli presented to human finger pad is often difficult in tactile texture studies. Both human texture perception and the physical stimuli presented to the skin are expressed as multidimensional information spaces. We developed a computational technique for matching these texture and physical stimulus spaces based on multivariate analysis approaches. The texture space is established via a semantic differential method. The physical space is based on vibrotactile spectrum information, one of the most commonly used principles for the analysis and artificial presentation of textures. The bases of the physical space were determined to ensure that the material allocations for the two spaces were similar, and we obtained well-matched spaces for 18 material samples. These successfully matched spaces will provide an analytic tool for material textures, and will help users of vibrotactile texture displays design virtual materials using adjectives or the names of materials.

Keywords : Haptics, Texture, Perceptual dimension

1. Introduction

A key challenge in tactile texture study is specifying the relationships between tactile sensations and stimuli. We investigated the linkage between vibrotactile stimuli and textures, considering that vibrotactile texture displays have been extensively studied by many researchers. Psychologists and neurophysiologists have also acknowledged the importance of vibrotactile signals in understanding human texture percepts. In particular, several research groups reported that the spectra of vibrotactile signals express human percepts of material surfaces. In the present study, we developed a computational technique to match vibrotactile spectra and material textures.

Vibrotactile texture displays are the most common tactile texture displays. These displays present the tactile sensations of materials by controlling the spectra or frequency components of vibrotactile stimuli [1]~[8]. However, the link between textures and vibrotactile stimuli has yet to be established.

The most frequently adopted vibrotactile display approach is a record-and-play method, in which the measured vibrotactile signals are replayed by texture displays after proper signal processing. For example, Yamamoto et al. transferred textures by measuring and replaying the vibratory signals generated upon contact between a tactile sensor and materials [9]. Similar approaches, i.e., the presentation of measured vibrotactile signals, have been widely used [3], [5], [7], [10]. These studies showed that material sensations can be successfully delivered by precisely replaying the previously measured vibrotactile stimuli. Naturally, the record-and-play method is unsuitable for creating or editing new textures.

In contrast, Konyo et al. studied the qualitative design of vibrotactile textures [4], [11]. They generated such textures by tuning three perceptual axes: roughness, hardness, and friction. This method enables users to create textures in accordance with human perception. However, the relationships between the perceptual axes and the vibrotactile stimuli were obtained from psychophysical experiments, rather than from the vibrotactile signals originating from the material samples. Hence, this method was suitable for synthesizing textures but did not aim at analyzing the vibrotactile signals generated by rubbing material surfaces.

Some studies have indicated a close relationship between the tactile sensations of material surfaces and the spectra of finger pad vibrations or deformations. For example, tactile differences in textures or vibrotactile stimuli correlate with the differences in the power or amplitude spectra of the skin vibrations generated when exploring such surfaces [12]~[14]. In

*1: Department of Mechanical Science and Engineering, Nagoya University. This work was supported in part by KAKENHI Shitsukan (23135514 & 25135717).

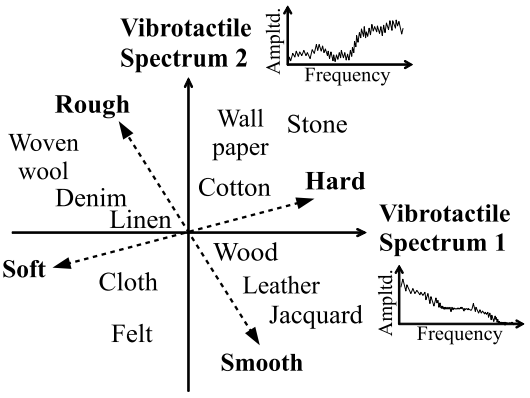

Fig. 1 Multidimensional space with tactile sensations (adjectives) and vibrotactile signals (spectra) of materials being matched.

addition, it was shown that roughness percepts are well represented by the weighted sum of the frequency spectra of the vibrotactile signals generated by rubbing material surfaces [15], [16]. Furthermore, Wiertlewski et al. showed that virtual materials can be presented by maintaining the spectra of the friction forces between the finger pad and the materials [5]. These studies made clear the importance of the spectra of vibrotactile signals for describing material textures. However, although a human tactile texture is intrinsically composed of multiple dimensions such as the roughness, hardness, and friction [17], few studies have investigated the relationships between the vibrotactile spectra and such textural multidimensionality.

In this study, we developed a method to match the qualitative representations of tactile sensation (texture space) and vibrotactile stimuli (physical space) in a multidimensional space, as shown in Fig. 1. The texture space is composed of adjectives that represent the qualities of tactile sensation, such as rough-smooth and hard-soft. The physical space is formed by the spectra of the vibrotactile signals. Materials are located in the matched space according to their vibrotactile signals and tactile sensations. Such matching is effective for the texture display and analysis of vibrotactile textures. For example, the vibrotactile stimulus for presenting a certain virtual texture can be known and specified without measuring the vibrotactile signals of the material using tactile sensors. Moreover, the tactile sensations of newly observed vibrotactile signals can be estimated by using the matched texture and vibrotactile spaces.

2. ESTABLISHMENT OF TEXTURE SPACE

The texture space is a multidimensional space based on adjectives related to the physical characteristics of materials such as rough and soft. The tactile sensations of materials are located in this space. Naturally, the perceptual space of the materials includes nonlinearity. However, a good starting point would be to hypothesize that the perceptual space is expressed by a linear synthesis of each adjective base. Actually, many researchers have attempted to identify the texture space using linear analysis techniques [17].

2.1 Methods and Materials

To establish the texture space, we use the semantic differential method, in which participants experience many material samples and perform sensory evaluations using adjectives representing tactile sensations. The materials are specified in an orthogonal space after a factor analysis is applied to the acquired subjective data. The bases of the orthogonal space are expressed by the synthesis of the adjectives. We constructed the texture space using the abovementioned procedure.

The materials included walnut wood, woven wood, a fake leather sheet (DI-NOC Film LE-137, 3M), oiled leather, embossed paper, jacquard, crinkled paper, Japanese paper, artificial grass, felt (long hair), felt (short hair), denim, a tablecloth, woven wool, cotton, linen, fine cloth, and uneven wallpaper, as shown in Fig. 2. All materials were cut into 50 mm $\times$ 50 mm pieces and attached to hard plastic plates using glue.

Five blindfolded volunteers who were not aware of the objectives of this study touched eighteen types of randomly presented materials and evaluated their textures using four types of paired bipolar adjectives: rough-smooth, bulky-flat, hard-soft, and sticky-slippery. These paired adjectives are considered to be the principal psychophysical dimensions for the tactile percepts of material surfaces [17]. Each pair was rated on a seven-point scale. The ratings of individual participants were normalized for each adjective pair. The averages among the participants were treated as the final values of the materials according to the following expression:

$$\boldsymbol{J} = (\boldsymbol{j}_1, \boldsymbol{j}_2, \cdots, \boldsymbol{j}_i, \cdots, \boldsymbol{j}_p), \quad (1)$$

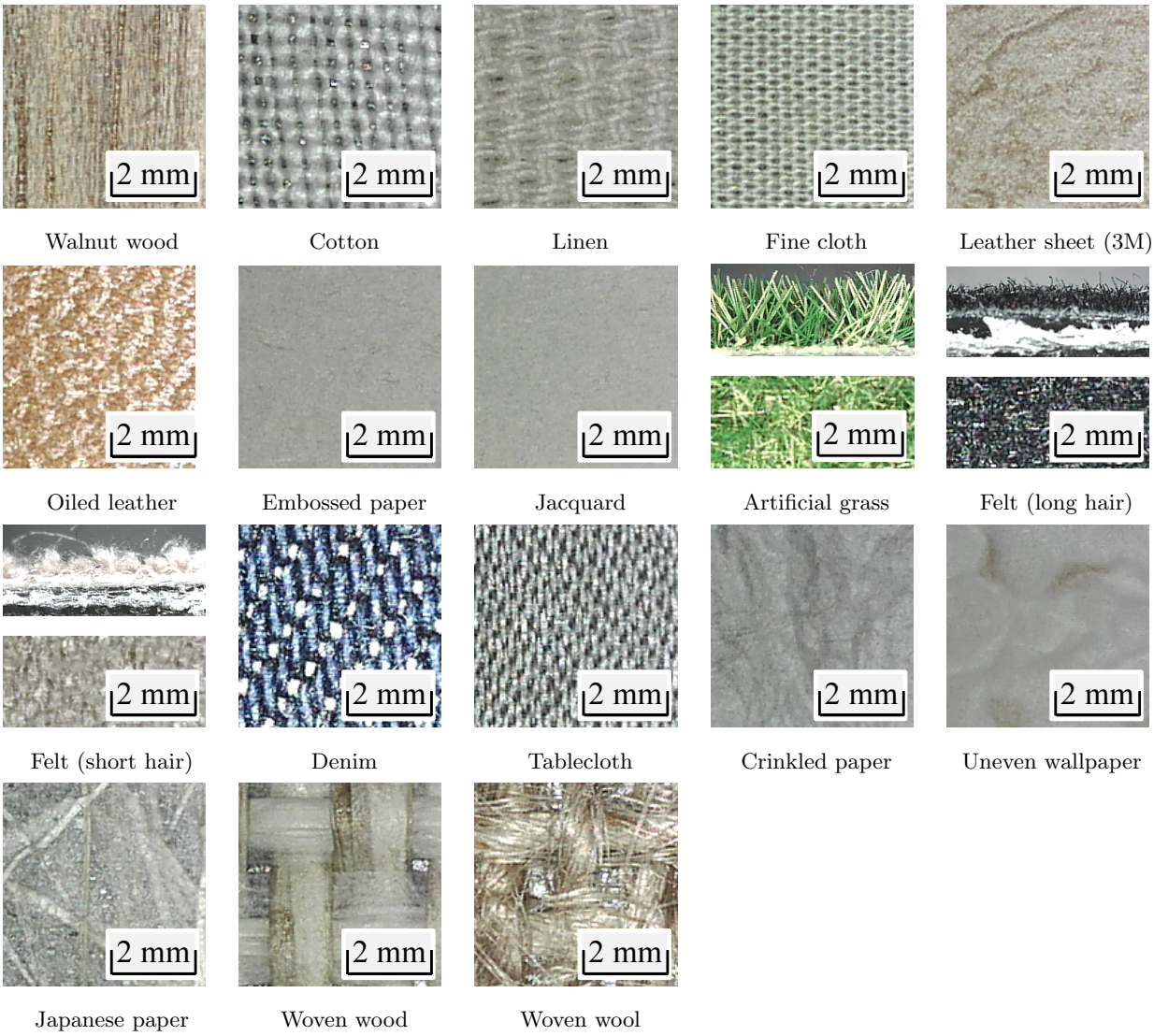

Fig. 2 Measured materials. Cross-sectional photos are also shown for the two types of felt and the artificial grass.

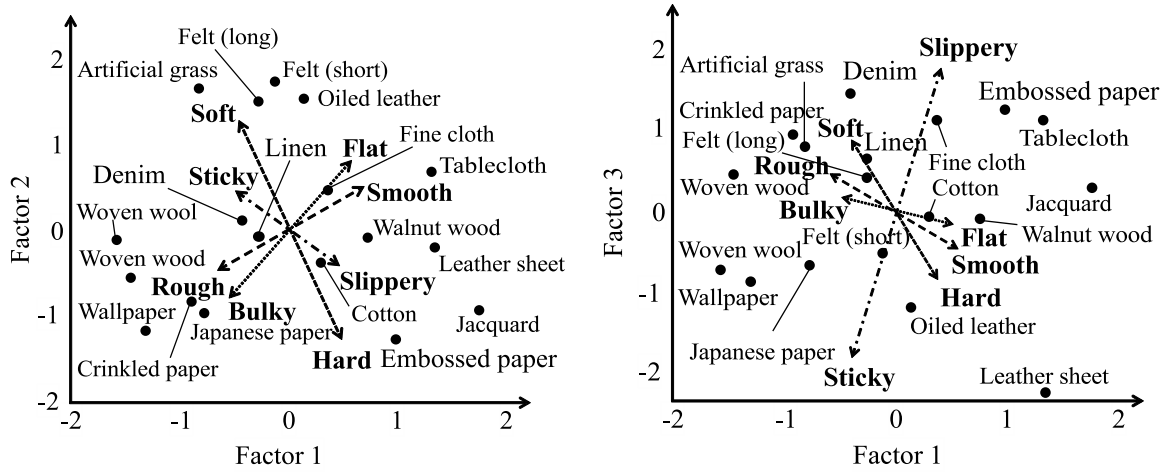

(a) Texture space of factors 1 and 2

(b) Texture space of factors 1 and 3

Fig. 3 Material distribution in texture space

Table 1 Loadings of three factors

	Factor 1	Factor 2	Factor 3
Rough/Smooth	0.90	0.29	-0.17
Bulky/Flat	0.76	0.49	-0.06
Hard/Soft	-0.61	0.77	0.31
Sticky/Slippery	0.62	-0.24	0.61
Contrbt. ratio	0.54	0.25	0.13

where i and p are the material number and number of materials, respectively. $\boldsymbol{j}_i$ is the column vector of average adjective values for material i, and described by

$$\boldsymbol{j}_i = (r_i, b_i, h_i, s_i)^T, \tag{2}$$

where r_i, b_i, h_i, and s_i are the scores of the rough-smooth, bulky-flat, hard-soft, and sticky-slippery sensations, respectively.

2. 2 Configured Texture Space

Figure 3 and Table 1 present the texture space and factor loadings configured by applying a factor analysis to the acquired subjective data. The analysis exhibited a three-factor model because the sum of the contribution ratios of these axes reached 0.92. The space contains four arrows that express each adjective pair. The tactile sensations vary with these arrows. The lengths of the axes reflect the gravity of each adjective pair on a plane. In the first-second-dimensional plane, the axes corresponding to hard-soft, rough-smooth, and bulky-flat are longer than the sticky-slippery axis, which indicates that the plane captures these features of the textures. In contrast, the third dimension clearly reflects the sensation of friction.

The locations or coordinates of materials in the three-dimensional space are

$$\boldsymbol{Y} = (\boldsymbol{y}_1,\ \boldsymbol{y}_2,\ \cdots,\ \boldsymbol{y}_p) = \boldsymbol{A}^+ \cdot \boldsymbol{J}, \tag{3}$$

where $\boldsymbol{y}_i = (y_{i1}, y_{i2}, y_{i3})^T$ and $\boldsymbol{A}$ indicate the coordinate of material i and a matrix of factor loadings as specified in Table 1, respectively.

3. ESTABLISHMENT OF VIBROTACTILE SPECTRUM SPACE

Here, we configure the space for the vibrotactile signals that occur when a probe scans material surfaces. The measurement of the vibrations and the computation of the subbands of the vibrotactile spectra are described in Sections 3. 1 and 3. 2, respectively. The computation of the vibrotactile spectra bases and their optimization appear in Sections 3. 3 and 3. 4, respectively.

3. 1 Measurement of Vibration of Contactor with Sustained Pressure

In tactile exploration, the finger pad deformations depend on the surface profile of the explored material. Some researchers have indirectly or directly measured such deformations. For example, Bensmaïa and Hollins measured the fingertip vibration when the finger pads rubbed materials by using a Hall-effect sensor and a magnet [16], or Doppler velocimeter [18]. Other researchers utilized sounds [19], [20], wave propagation through the skin [21], or frictional forces [5], [22], [23] to analyze or measure the finger pad vibrations caused by material surfaces. Given that these studies adopted indirect measurement approaches, clearly, directly measuring a finger pad's deformation due to a material surface is difficult. One successful direct measurement method involved the observation of the contact area between a finger pad and a glass surface using a high-speed camera [24]; however, this approach is available only for transparent materials.

Instead of using real finger pad deformations, we measured the vibrations of a metal contactor with a load of 1.2 N, i.e., the typical human force during a tactile exploration. The contactor has a rigid hemisphere with a radius of 4 mm, and it was moved horizontally using a linear robotic arm by way of a rigid link and rotational joint. Each material was measured five times along randomly selected 100-mm paths, with a scanning speed of 20 mm/s. The contactor displacements were measured using a laser displacement sensor (CD5-30, OPTEX FA Co., Kyoto, Japan), with the spatial and temporal resolutions set to 0.02 μm and 1250 Hz, respectively.

3. 2 Subbands of Spectra

As previously discussed, the vibrotactile spectrum of each material expresses its tactile sensation. Naturally, a single spectrum includes many wave components. We divided each spectrum into subbands to reduce the number of such variables and facilitate effective searching using a computer. Some researchers have shown that accurate spectrum representations are unnecessary for vibrotactile textures, which allows a drastic decrease in the number of the variables [25]. For example, the sum of the energies of frequency-shaped or weighted spectrum well represents the perceived roughness of a texture [13], [15], [16]. In the light of these facts, the

present study treated the spectra averaged in a limited frequency band. Such subbands of the spectra are then regarded as the base vectors of the vibrotactile spectrum space.

The subband vectors were calculated as follows. The amplitude spectra were computed from the vibrotactile signals of each material obtained in Section 3. 1. For each material, the spectra from five measurements were averaged. The frequency bands of 0–500 Hz were divided into ten subbands, and the average of the amplitude spectra was calculated within each subband. The average of the amplitudes in the jth subband for material i was determined as follows:

$$a_{ij} = \int_{f_{j-1}}^{f_j} \frac{a_i(f)}{f_j - f_{j-1}} df \quad (4)$$
$$(j = 1, \cdots, 10;\ f_j < f_{j+1}, f_0 = 0, f_{10} = 500),$$

where f and $a_i(f)$ are the frequency and amplitude of f, respectively. Then, a_{ij} are standardized among materials for each j. The subband vector of material i is expressed as follows:

$$\boldsymbol{s}_i = (a_{i1},\ a_{i2},\ \cdots,\ a_{i10})^T. \quad (5)$$

The subband vectors of all the materials are expressed in the form of a matrix:

$$\boldsymbol{S} = (\boldsymbol{s}_1,\ \boldsymbol{s}_2,\ \cdots,\ \boldsymbol{s}_p). \quad (6)$$

A search is made for subband widths (f_0–f_{10}) to find a match between the texture and vibrotactile spaces, as mentioned in Section 3. 4.

3. 3 Computation of Vibrotactile Spectrum Bases

We determine the vibrotactile spectrum space to express the tactile sensations of materials. In particular, we compute the bases of the spectrum space ($\boldsymbol{B}$) such that the spectra of the materials ($\boldsymbol{S}$) well express the allocations of the materials in the texture space ($\boldsymbol{Y}$).

The bases of the vibrotactile space are computed by

$$\boldsymbol{B} = \boldsymbol{Y} \cdot \boldsymbol{S}^{+}. \quad (7)$$

where $\boldsymbol{B}$ is a 3 (number of dimensions of texture space) × 10 (number of subbands) matrix. The row vectors of this matrix represent the bases of the vibrotactile spectrum space. In other words, $\boldsymbol{B}$ is a projection from $\boldsymbol{S}$ (vibrotactile signals of materials) to $\boldsymbol{Y}$ (their locations in the textural space) because $\boldsymbol{Y} = \boldsymbol{B} \cdot \boldsymbol{S}$.

3. 4 Search for Vibrotactile Spectrum Bases

Using the following procedures, we optimize the subband widths f_0–f_{10} such that the vibrotactile spectra specify the tactile sensations of materials.

We exhaustively set the widths of ten subbands. Narrow bandwidths are set for the lower frequency bands, whereas wide bandwidths are used for higher-frequency bands, considering the frequency response characteristics of the mechanical receptors. Some researchers have used receptor filters to establish the validity of setting bandwidths according to receptor characteristics [16], [26], [27]. One of the major bases of such ideas is that the roles and information processes of each receptor class are independent in the perception of texture or vibrotactile stimuli [28]~[31]. In the low frequency bands, the sensitivities of Meissner's and Merkel's corpuscles to vibrotactile stimuli are better than those of the other corpuscles. The active bandwidths of these corpuscles are relatively narrow. In the high frequency bands (more than 100 Hz), the sensitivity of Pacinian corpuscles is extremely high.

1. Here, $f_0 = 0$, $f_{10} = 500$, and f_i values are natural numbers between 0 and 500.
   $f_1 = f_0 + \{1, 2, ..., 10\}$,
   $f_2 = f_1 + \{1, 2, ..., 20\}$,
   $f_3 = f_2 + \{1, 2, ..., 20\}$,
   $f_4 = f_3 + \{5, 10, ..., 50\}$,
   $f_5 = f_4 + \{5, 10, ..., 50\}$,
   $f_6 = f_5 + \{5, 10, ..., 50\}$,
   $f_7 = f_6 + \{10, 20, ..., 100\}$,
   $f_8 = f_7 + \{10, 20, ..., 100\}$,
   and $f_9 = f_8 + \{10, 20, ..., 100\}$.
2. Using the ten subbands determined in the above step, the subband vectors $\boldsymbol{S}$ of the materials are computed using (4), (5), and (6).
3. Using $\boldsymbol{S}$, (3), and (7), the coordinates of the materials in the vibrotactile spectrum space are determined by
   $$\hat{\boldsymbol{Y}} = \boldsymbol{B} \cdot \boldsymbol{S}. \quad (8)$$
4. The error between $\boldsymbol{Y}$ and $\hat{\boldsymbol{Y}}$ is computed using the following expression:
   $$\sum ||\boldsymbol{y}_i - \hat{\boldsymbol{y}}_i||. \quad (9)$$

After repeating these procedures, we adopted the subband widths with the minimum error value.

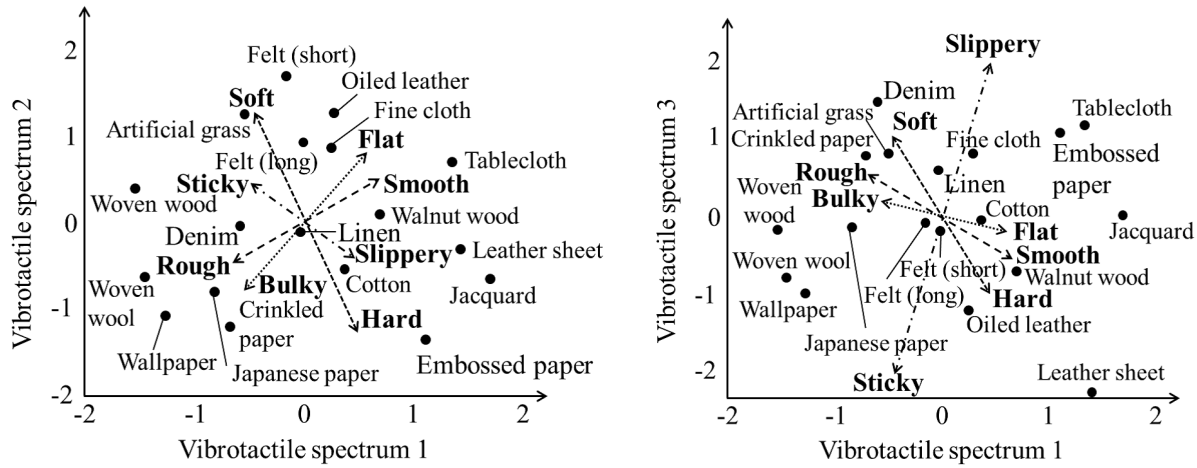

(a) Physical space of spectra 1 and 2 (b) Physical space of spectra 1 and 3

Fig. 4 Material distribution in vibrotactile space

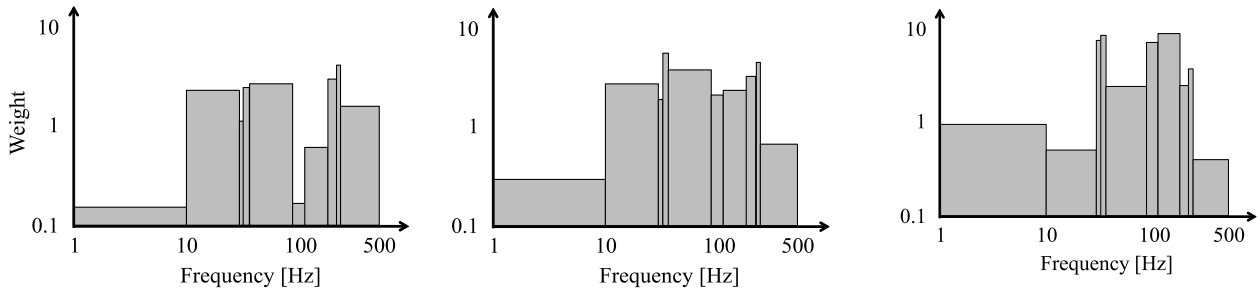

(a) Weights of subbands: Spectrum 1. (b) Weights of subbands: Spectrum 2. (c) Weights of subbands: Spectrum 3.

Fig. 5 Absolute components of $\boldsymbol{B}$ matrix. Ensembles of frequency subbands for each vibrotactile spectrum basis.

Table 2 Subband frequencies

Frequencies for subbands	f_0	f_1	f_2	f_3	f_4	f_5	f_6	f_7	f_8	f_9	f_{10}
[Hz]	0	10	30	32	37	87	112	182	222	232	500

4. MATCHED VIBROTACTILE SPACE AND ITS VALIDATION

4.1 Vibrotactile Space Matched with Texture Space

Figure 4 shows the vibrotactile space established in Section 3. Eighteen types of materials and four axes for adjectives are also located in this space. This space connects the tactile sensations that humans experience and the vibrotactile signals acquired by rubbing materials.

Figure 5 shows $\boldsymbol{B}$, the structures of the individual vibrotactile spectrum axes. The structures of the axes are expressed as the weights of the vibrotactile spectra's subbands, of which the widths are summarized in Table 2. On the first axis, the 10–90 Hz and 182–500 Hz frequency ranges were highly loaded. On the second axis, the 10–232 Hz frequencies were loaded. The third axis weighted the band up to 10 Hz and at 30–232 Hz. However, because the orthogonal rotation of the vibrotactile space is indeterminant, it should be noted that the subband structures do not always show profiles similar to those acquired here.

4.2 Validation: Comparison of Estimated and Observed Adjective Scores

We investigated the extent to which the estimated adjective scores described the observed adjective scores. In other words, we tested how accurately the vibrotactile signals of the materials could estimate their sensory properties. The adjective scores estimated from the vibrotactile signals are expressed as follows:

$$\hat{\boldsymbol{J}} = \boldsymbol{A} \cdot \hat{\boldsymbol{Y}}. \tag{10}$$

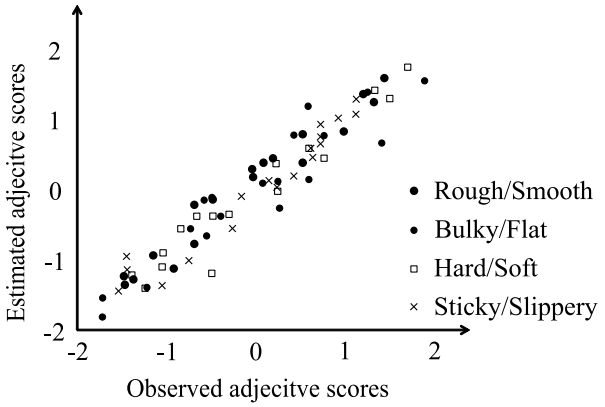

Fig. 6 Variances of observed and estimated adjective scores of 18 materials.

We then compared $\boldsymbol{J}$ and $\hat{\boldsymbol{J}}$, which are the observed and estimated adjective scores of materials, respectively.

Figure 6 shows the comparison of the observed and estimated adjective scores for each of the eighteen materials. For the adjective pairs of rough-smooth, bulky-flat, hard-soft, and sticky-slippery, the R^2 values of $\boldsymbol{J}$ and $\hat{\boldsymbol{J}}$ were 0.94, 0.95, 0.89, and 0.92, respectively. Approximately, 90% of the adjective scores of the materials were expressed by their vibrotactile spectra.

We investigated the errors between the estimated and observed adjective scores for each material. We computed $\hat{\boldsymbol{J}} - \boldsymbol{J}$, and then determined the errors for each adjective pair. In light of the effect size in statistics [32], the substantial effect of the errors was regarded small when these errors were at most 30% of the standard deviation (1.0) of the observed adjective scores.

The $\hat{\boldsymbol{J}} - \boldsymbol{J}$ values are listed in Table 3. The gray entries indicate that the errors between the observed and the estimated adjective scores are more than 30% of the standard deviation of the observed scores. The adjective scores of the walnut wood, cotton, leather sheet, embossed paper, jacquard, felt (short hair), tablecloth, and uneven wallpaper were well estimated. However, the adjective scores of the fine cloth, artificial grass, felt (long hair), woven wood, and woven wool were not well estimated. In particular, the estimation errors in the cases of these materials were greater than 30% for the adjective pair hard-soft. For eight of the 18 materials, the errors in the hard-soft scores were non-negligible, whereas just a few materials exhibited high errors for the other scores. These results indicate that the vibrotactile approach of the present study is limited in terms of presenting the perceived softness or hardness of materials.

These comparisons showed that the texture and vibrotactile spectra spaces were fairly matched using the method considered in the present study. The variations in the adjective scores were represented by the vibrotactile spectra with accuracies higher than 90% with the hard-soft scores being an exception. As discussed in Section 5. 1, the hard-soft properties of the materials were represented poorly compared with the other sensory properties as a result of the specifications of the vibrotactile signals. Furthermore, for some materials, the errors in their roughness, bulkiness, and stickiness scores were substantial. Such errors may stem from limitations of the vibrotactile signal measurement setup, as discussed in Section 5. 2.

5. DISCUSSION

5. 1 Vibrotactile Stimuli are Weak in Presentation of Hardness and Softness of Materials

The present study suggested that the vibrotactile signals are limited in terms of presenting the softness percepts of materials. These aspects of the hard-soft scores reflect the fact that the perception of material compliance is not generally based on the vibrotactile signals, although the perceptions of the surface roughness [15], [28] and frictional characteristics of materials [33], [34] are linked with the vibrotactile signals of finger pads. The perception of surface compliance is attributed to the pressure distribution within the contact area between the finger pad and the material during pushing motion [35], [36]. The vibrotactile stimuli do not capture information such as the pressure distributions and contact areas. However, the goodness of fit of the hard-soft scores was as high as 0.89, which indicates that the softness percepts were partly presented by the vibrotactile signals. Very recently, some studies showed the connections between the vibrotactile stimuli and the softness percept of materials [4], [37]~[40]. The mechanism of the vibrotactile softness display phenomenon remains to be clarified, but the results of the present study are in harmony with those of other recent reports.

Table 3 Errors between estimated and observed adjective scores: $\hat{\boldsymbol{J}} - \boldsymbol{J}$. Gray cells indicate substantial errors. Positive values indicate that the materials were estimated rougher, bulkier, harder, or stickier than reported in sensory evaluation.

	Rough/Smooth	Bulky/Flat	Hard/Soft	Sticky/Slippery
Walnut wood	-0.2494	0.1174	-0.1501	0.2642
Cotton	-0.2200	0.2168	0.1051	-0.1200
Linen	-0.3215	-0.0449	0.1426	-0.1227
Fine cloth	-0.2831	0.0565	-0.3274	0.3680
Leather sheet	-0.1253	0.0907	0.0918	-0.0887
Oiled leather	0.1603	-0.1520	0.3236	-0.1242
Embossed paper	-0.2291	0.0293	0.1922	-0.0277
Jacquard	-0.1503	-0.0482	-0.1708	0.2501
Artificial grass	-0.4714	0.2682	0.3889	-0.3312
Felt (long hair)	-0.3104	0.2010	0.7688	0.0623
Felt (short hair)	0.1634	0.0332	-0.1173	-0.2611
Denim	0.0918	0.3171	0.0147	0.0590
Tablecloth	0.1041	-0.1429	0.0322	-0.0488
Crinkled paper	0.1875	-0.2740	0.5300	-0.1231
Japanese paper	-0.1813	0.2747	-0.4044	-0.2767
Woven wood	-0.2405	-0.4632	-0.5761	0.6946
Woven wool	-0.1162	0.3338	0.4624	-0.1820
Uneven wallpaper	-0.0733	-0.0926	-0.0019	0.0807

5. 2 Limitations of Vibrotactile Signal Measurements

The rough-smooth, bulky-flat, and sticky-slippery properties were well represented by the vibrotactile spectra, but the errors of these properties were non-negligible for a few materials. This is potentially due to limitations in measurement setup for the vibrotactile signals.

For example, the error between the estimated and observed rough-smooth scores for artificial grass was -0.47, which indicated that it was estimated to be much smoother than it actually was. Artificial grass has fine cilia on its surface, for which epidermal ridges or fingerprints may play an important role in increasing the perception of roughness [23], [41], [42]. On the other hand, under our measurement setup, the surface of the measurement contactor was hard and smooth, and could not capture the roughness percepts caused by these cilia.

Similarly, woven wood was estimated to be flatter and stickier than the corresponding human sensory evaluation. This material was a woven sheet of thin wood strips. When this material was touched with a finger pad, an uneven pressure or deformation occurred at the contact area. This unevenness produced macroscopic roughness percepts expressed as "bulky." The measurement setup that was used did not find the stimulus distribution on the contact area, and the bulkiness properties of the woven wood were not fully described. Furthermore, the vibrotactile signals included frictional vibrations that were not differentiated from those caused by surface roughness. This might have led to the error in the estimated stickiness of the material.

Some may speculate that the use of tactile sensors mimicking a human finger would improve the vibrotactile measurement. Artificial finger sensors can have several transducers spread within a soft superficial layer. However, one of the major flaws of such sensors is their frictional properties. Even generating their comprehensive friction properties, which can be represented by friction coefficients, similar to those of human fingers, is highly demanding [43], [44]. It is more difficult to develop tactile sensors that reproduce frictional properties dynamically, similar to those of human fingers.

6. CONCLUSION

This study developed a technique for matching the textures and vibrotactile signals of materials in a multidimensional space. Such a space can be helpful for the analysis and display of vibrotactile textures considering that human textural percepts are multidimensional. In contrast, earlier studies mainly dealt with unidimensional matching.

The texture space was established based on the sensory evaluation of material samples and factor analysis. The vibrotactile space was constructed based on the subbands of the spectra of vibrotac-

tile signals that were generated as a result of explorative contact between material surfaces and a spherical contactor. The bases of the vibrotactile space were determined based on the similarity between the locations of the materials in the two spaces. Therefore, the established vibrotactile spectra space described the sensory scores of materials with accuracies of approximately 90%, although limitations were found in the representation of the perceived hardness or softness of materials. In addition, the method to measure vibrotactile signals should be improved for better representation of textures. The developed method of connecting textures and vibrotactile stimuli is generally applicable to vibrotactile texture displays with a single vibratory source or contactor, which are likely to be commercially available, and will help in the analysis of human percepts of vibrotactile textures.

Reference

[1] M. Konyo, S. Tadokoro, T. Takamori, and K. Oguro, Artificial tactile feel display using soft gel actuators; *Proceedings of IEEE International Conference on Robotics and Automation*, pp. 3416–3421 (2000).

[2] D. Allerkamp, G. Böttcher, F.-E. Wolter, A. C. Brady, J. Qu, and I. R. Summers, A vibrotactile approach to tactile rendering; *Visual Computer*, vol. July, pp. 97–108 (2006).

[3] M. Germani, M. Mengoni, and M. Peruzzini, Electro-tactile device for material texture simulation; *International Journal of Advanced Manufacturing Technology*, vol. 68, no. 9-12, pp. 2185–2203 (2013).

[4] T. Yamauchi, S. Okamoto, M. Konyo, Y. Hidaka, T. Maeno, and S. Tadokoro, Real-time remote transmission of multiple tactile properties through master slave robot system; *Proceedings of IEEE International Conference on Robotics and Automation*, pp. 1753–1760 (2010).

[5] M. Wiertlewski, J. Losada, and V. Hayward, The spatial spectrum of tangential skin displacement can encode tactual texture; *IEEE Transactions on Robotics*, vol. 27, no. 3, pp. 461–472 (2011).

[6] Y. Matsuura, S. Okamoto, S. Asano, H. Nagano, and Y. Yamada, A method for altering vibrotactile textures based on specified materials; *Proceedings of IEEE International Symposium on Robot and Human Interactive Communication*, pp. 1007–1012 (2012).

[7] H. Culbertson, J. Unwin, B. E. Goodman, and K. J. Kuchenbecker, Generating haptic texture models from unconstrained tool-surface interactions; *Proceedings of IEEE World Haptics Conference*, pp. 295–300 (2013).

[8] S. Saga and R. Raskar, Simultaneous geometry and texture display based on lateral force for touchscreen; *Proceedings of IEEE World Haptics Conference*, pp. 437–442 (2013).

[9] A. Yamamoto, S. Nagasawa, H. Yamamoto, and T. Higuchi, Electrostatic tactile display with thin film sliderand its application to tactile telepresentation systems; *IEEE Transactions on Visualization and Computer Graphics*, vol. 12, no. 2, pp. 168–177 (2006).

[10] S. Okamoto, M. Konyo, T. Maeno, and S. Tadokoro, Remote tactile transmission with time delay for robotic master-slave systems; *Advanced Robotics*, vol. 25, no. 9–10, pp. 1271–1294 (2011).

[11] M. Konyo, A. Yoshida, S. Tadokoro, and N. Saiwaki, A tactile synthesis method using multiple frequency vibration for representing virtual touch; *Proceedings of IEEE/RSJ International Conference on Intelligent Robots and Systems*, pp. 3965–3971 (2005).

[12] S. Bensmaïa, M. Hollins, and J. Yau, Vibrotactile intensity and frequency information in the pacinian system: A psychophysical model; *Perception and Psychophysics*, vol. 67, no. 5, pp. 828–841 (2005).

[13] S. Okamoto and Y. Yamada, An objective index that substitute quality of vibrotactile material-like texture; *Proceedings of IEEE/RSJ International Conference on Intelligent Robots and Systems*, pp. 3060–3067 (2011).

[14] S. Okamoto, S. Ishikawa, H. Nagano, and Y. Yamada, Spectrum-based synthesis of vibrotactile stimuli: Active footstep display for crinkle of fragile structures; *Virtual Reality*, vol. 17, no. 3, pp. 181–191 (2013).

[15] W. M. Bergmann Tiest and A. M. Kappers, Haptic and visual perception of roughness; *Acta Psychologica*, vol. 124, pp. 177–189 (2007).

[16] S. Bensmaïa and M. Hollins, Pacinian representations of fine surface texture; *Perception and Psychophysics*, vol. 67, no. 5, pp. 842–854 (2005).

[17] S. Okamoto, H. Nagano, and Y. Yamada, Psychophysical dimensions of tactile perception of textures; *IEEE Transactions on Haptics*, vol. 6, no. 1, pp. 81–93 (2013).

[18] A. I. Webera, H. P. Saala, J. D. Lieberb, J.-W. Chenga, L. R. Manfredia, J. F. Dammann III, and S. J. Bensmaïa, Spatial and temporal codes mediate the tactile perception of natural textures; *PNAS*, vol. 110, no. 42, pp. 17107–17112 (2013).

[19] S. Guest, C. Catmur, D. Lloyd, and C. Spence, Audiotactile interactions in roughness perception; *Experimental Brain Research*, vol. 146, no. 2, pp. 161–171 (2002).

[20] Y. Tanaka, Y. Horita, A. Sano, and H. Fujimoto, Tactile sensing utilizing human tactile perception; *Proceedings of IEEE World Haptics Conference*, pp. 621–626 (2011).

[21] Y. Tanaka, Y. Horita, and A. Sano, Fingermounted skin vibration sensor for active touch; *Proceedings of Eurohaptics*, pp. 169–174 (2012).

[22] A. M. Smith, C. E. Chapman, M. Deslandes, J. S. Langlais, and M. P. Thibodeau, Role of friction and tangential force variation in the subjective scaling of tactile roughness; *Experimental Brain Research*, vol. 144, no. 2, pp. 211–223 (2002).

[23] R. Fagiani, F. Massi, E. Chatelet, Y. Berthier, and A. Akay, Tactile perception by friction induced vibrations; *Tribology International*, vol. 44,

pp. 1100–1110 (2011).
[24] V. Levesque and V. Hayward, Experimental evidence of lateral skin strain during tactile exploration; *Proceedings of Eurohaptics*, pp. 261–275 (2003).
[25] S. Okamoto and Y. Yamada, Lossy data compression of vibrotactile material-like textures; *IEEE Transactions on Haptics*, vol. 6, pp. 69–80 (2013).
[26] A. Israr, H. Z. Tan, J. Mynderse, and G. T. Chiu, A psychophysical model of motorcycle handlebar vibrations; *Proceedings of ASME International Mechanical Engineering Congress and Exposition*, vol. 9, pp. 1233–1239 (2007).
[27] J. C. Makous, R. M. Friedman, and J. Charles J. Vierck, A critical band filter in touch; *Neuroscience*, vol. 15, pp. 2808–2818 (1995).
[28] C. E. Connor, S. S. Hsiao, J. R. Phillips, and K. O. Johnson, Tactile roughness: Neural codes that account for psychophysical magnitude estimates; *Journal of Neuroscience*, vol. 10, no. 12, pp. 3823–3836 (1990).
[29] M. Hollins and S. R. Rinser, Evidence for the duplex theory of tactile texture perception; *Attention, Perception & Psychophysics*, vol. 62, no. 4, pp. 695–705 (2000).
[30] G. A. Gescheider, R. T. Verrillo, and C. L. van Doren, Prediction of vibrotactile masking ffunctions; *Journal of Acoustical Society of America*, vol. 72, pp. 1421–1426 (1982).
[31] M. Hollins, S. J. Bensmaiä, and S. Washburn, Vibrotactile adaptation impairs discrimination of fine, but not coarse, textures; *Somatosensory & Motor Research*, vol. 18, no. 4, pp. 253–262 (2001).
[32] J. Cohen, *Statistical Power Analysis for the Behavioral Sciences*. Lawrence Erlbaum Assoc Inc. (1988).
[33] Y. Nonomura, T. Fujii, Y. Arashi, T. Miura, T. Maeno, K. Tashiro, Y. Kamikawa, and R. Monchi, Tactile impression and friction of water on human skin; *Colloids and Surfaces B: Biointerfaces*, vol. 69, pp. 264–267 (2009).
[34] M. Konyo, H. Yamada, S. Okamoto, and S. Tadokoro, Alternative display of friction represented by tactile stimulation without tangential force; *Proceedings of EuroHaptics*, pp. 619–629 (2008).
[35] A. Bicchi, E. P. Schilingo, and D. De Rossi, Haptic discrimination of softness in teleoperation:the role of the contact area spread rate; *IEEE Transactions on Robotics & Automation*, vol. 16, no. 5, pp. 496–504 (2000).
[36] K. Fujita and H. Ohmori, A new softness display interface by dynamic fingertip contact area control; *Proceedings of 5th World Multiconference on Systemics Cybernetics and Informatics*, pp. 78–82 (2001).
[37] L. B. Porquis, M. Konyo, and S. Tadokoro, Representation of softness sensation using vibrotactile stimuli under amplitude control; *IEEE International Conference on Robotics and Automation*, pp. 1380–1385 (2011).
[38] Y. Visell, B. L. Giordano, G. Millet, and J. R. Cooperstock, Vibration influences haptic perception of surface compliance during walking; *Plos one*, vol. 6, no. 3, p. e17697 (2011).
[39] A. Ikeda, T. Suzuki, J. Takamatsu, and T. Ogasawara, Producing method of softness sensation by device vibration; *Proceedings of the IEEE International Conference on Systems, Man, and Cybernetics*, pp. 3384–3389 (2013).
[40] J. Lang and S. Andrews, Measurement-based modeling of contact forces and textures for haptic rendering; *IEEE Transactions on Visualization and Computer Graphics*, vol. 17, no. 3, pp. 385–391 (2011).
[41] Y. Mukaibo, H. Shirado, M. Konyo, and T. Maeno, Development of a texture sensor emulating the tissue structure and perceptual mechanism of human fingers; *Proceedings of IEEE International Conference on Robotics and Automation*, pp. 2565–2570 (2005).
[42] J. Scheibert, S. Leurent, A. Prevost, and G. Debr'egeas, The role of fingerprints in the coding of tactile information probed with a biomimetic sensor; *Science*, vol. 323, no. 5920, pp. 1503–1506 (2009).
[43] M. Tomimoto, The frictional pattern of tactile sensations in anthropomorphic fingertip; *Tribology International*, vol. 44, pp. 1340–1347 (2011).
[44] F. Shao, T. H. Childs, and B. Henson, Developing an artificial fingertip with human friction properties; *Tribology International*, vol. 42, pp. 1575–1581 (2009).

(received Jan. 15, 2014)

Biography

Yoichiro Matsuura

is a mechanical engineer who received B.S. and M.S. degrees in engineering from Nagoya University in 2012 and 2014, respectively. His study interests include human-computer interfaces.

Shogo Okamoto (Member)

received M.S. and Ph.D. degrees in information sciences in 2007 and 2010, respectively, from the Graduate School of Information Sciences, Tohoku University. Since 2010, he has been an assistant professor at the Graduate School of Engineering, Nagoya University. His research interests include haptic interfaces and human-assistive technology.

Hikaru Nagano

received B.S. and M.S. degrees in engineering from Nagoya University in 2010 and 2012, respectively. Currently, he is a Ph.D. candidate in the Department of Mechanical Science and Engineering, Nagoya University. He has also received the JSPS fellowship for young researchers since 2013. His research interests include human perception.

Yoji Yamada

received a Ph.D. degree from the Tokyo Institute of Technology in 1990. He has been an associate professor at the Toyota Technological Institute, Japan since 1983. In 2004, he joined the National Institute of Advanced Industrial and Science Technology (AIST), as a group leader of the Safety Intelligence Research Group at the Intelligent Systems Research Institute. In 2008, he moved to the Graduate School of Engineering, Nagoya University, as a professor.